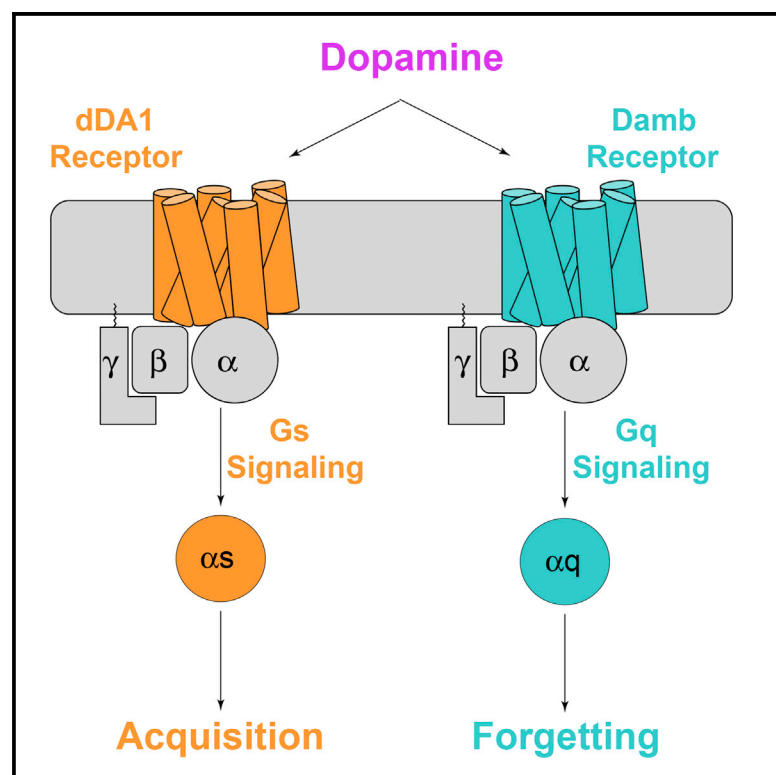


# Cell Reports

## Dopamine Receptor DAMB Signals via Gq to Mediate Forgetting in *Drosophila*

### Graphical Abstract



### Authors

Sophie Himmelreich, Ikuo Masuho, Jacob A. Berry, Courtney MacMullen, Nickolas K. Skamangas, Kirill A. Martemyanov, Ronald L. Davis

### Correspondence

kirill@scripps.edu (K.A.M.),  
rdavis@scripps.edu (R.L.D.)

### In Brief

Himmelreich et al. examine how mushroom body neurons discriminate signals for acquisition and forgetting, both mediated by dopamine. The authors show that acquisition is mediated by the dopamine receptor dDA1 coupled to Gs signaling. Forgetting is mediated by the dopamine receptor Damb coupled to Gq.

### Highlights

- The dopamine receptor dDA1 couples to Gs for intracellular signaling
- The dopamine receptor Damb couples to Gq for intracellular signaling
- $G\alpha q$  knockdown with RNAi in the mushroom bodies inhibits forgetting
- Dopamine spurs acquisition through dDA1/Gs and forgetting through Damb/Gq



# Dopamine Receptor DAMB Signals via Gq to Mediate Forgetting in *Drosophila*

Sophie Himmelreich,<sup>1,2</sup> Ikuo Masuho,<sup>1,2</sup> Jacob A. Berry,<sup>1</sup> Courtney MacMullen,<sup>1</sup> Nickolas K. Skamangas,<sup>1</sup> Kirill A. Martemyanov,<sup>1,3,\*</sup> and Ronald L. Davis<sup>1,3,4,\*</sup>

<sup>1</sup>Department of Neuroscience, The Scripps Research Institute Florida, Jupiter, FL 33458, USA

<sup>2</sup>These authors contributed equally

<sup>3</sup>Senior author

<sup>4</sup>Lead Contact

\*Correspondence: [kirill@scripps.edu](mailto:kirill@scripps.edu) (K.A.M.), [rdavis@scripps.edu](mailto:rdavis@scripps.edu) (R.L.D.)

<https://doi.org/10.1016/j.celrep.2017.10.108>

## SUMMARY

Prior studies have shown that aversive olfactory memory is acquired by dopamine acting on a specific receptor, dDA1, expressed by mushroom body neurons. Active forgetting is mediated by dopamine acting on another receptor, Damb, expressed by the same neurons. Surprisingly, prior studies have shown that both receptors stimulate cyclic AMP (cAMP) accumulation, presenting an enigma of how mushroom body neurons distinguish between acquisition and forgetting signals. Here, we surveyed the spectrum of G protein coupling of dDA1 and Damb, and we confirmed that both receptors can couple to Gs to stimulate cAMP synthesis. However, the Damb receptor uniquely activates Gq to mobilize Ca<sup>2+</sup> signaling with greater efficiency and dopamine sensitivity. The knockdown of Gαq with RNAi in the mushroom bodies inhibits forgetting but has no effect on acquisition. Our findings identify a Damb/Gq-signaling pathway that stimulates forgetting and resolves the opposing effects of dopamine on acquisition and forgetting.

## INTRODUCTION

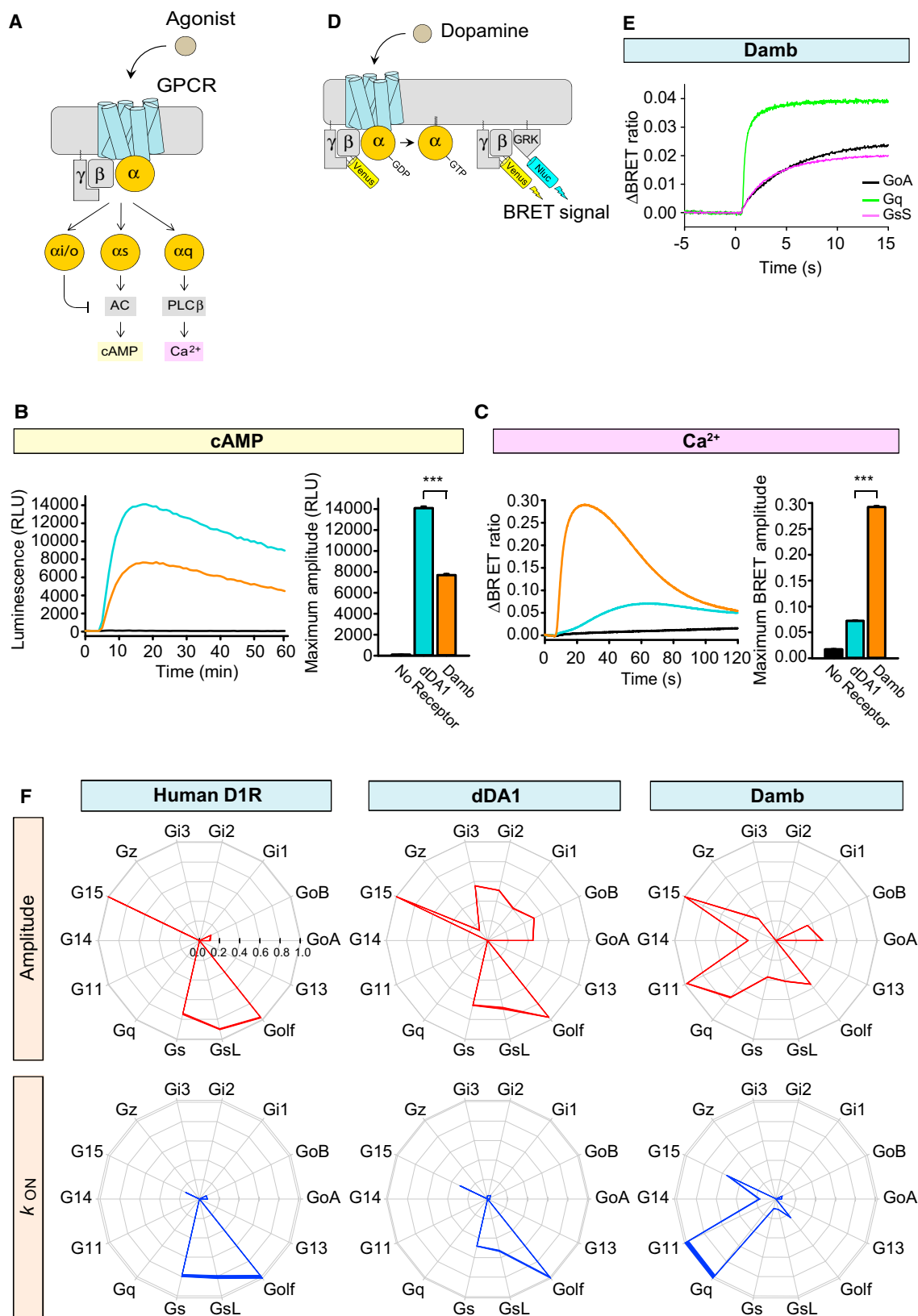
Pioneering neuroscience studies using *Drosophila melanogaster* have revealed that the brain is constructed with cellular and circuit mechanisms that promote forgetting (Davis and Zhong, 2017). The best-understood mechanism for active forgetting of olfactory memory at the circuit level involves the release of dopamine (DA) from dopaminergic neurons (DANs, forgetting cells) of the PPL1 cluster onto the axons of mushroom body neurons (MBNs, engram cells). Forgetting cells exhibit chronic activity (Berry et al., 2012) that slowly promotes forgetting, but they are stimulated by sensory information and quieted by sleep (Berry et al., 2015). DA released from the forgetting cells stimulates a specific DA receptor, dopamine receptor expressed in mushroom bodies (Damb), required for normal forgetting (Han et al., 1996; Berry et al., 2012). This receptor mobilizes an intracellular signaling pathway that includes the scaffolding protein Scribble and its associated protein components, Rac1 and Cofilin, that

may cause forgetting by reversing changes in the neuronal actin cytoskeleton that occur with memory formation (Davis and Zhong, 2017).

Curiously, several studies have shown that DA released from the PPL1 DANs is also required for the acquisition of new, aversive olfactory memories (Schwaerzel et al., 2003; Schroll et al., 2006; Claridge-Chang et al., 2009; Aso et al., 2012). The current working model envisions the unconditioned stimulus (US) for olfactory classical conditioning as conveyed by DAN activation of the MBNs. How DAN stimulation of MBNs might lead to both acquisition and forgetting of olfactory memories can be partially explained by the existence of a second DA receptor, named dDA1, which, like Damb, is preferentially and uniformly expressed along the axons of the MBNs, as revealed by light microscopic immunohistochemistry (Han et al., 1996; Kim et al., 2003). Mutants of dDA1 fail to acquire memory (Kim et al., 2007), consistent with a two-receptor model in which the dDA1 receptor mediates the acquisition of olfactory memories by MBNs and Damb spurs forgetting (Berry et al., 2012).

However, a two-receptor model presents a mystery of how MBNs know whether they are receiving an acquisition or forgetting signal from the PPL1 DANs. The most attractive explanation for this is that the two receptors might have different signaling properties and mobilize distinct signaling cascades. However, prior pharmacological characterization experiments in reconstituted systems classified both receptors as D1-like, stimulating the accumulation of cyclic AMP (cAMP) by activating the heterotrimeric G protein Gs and the effector adenylyl cyclase (Sugamori et al., 1995; Han et al., 1996; Reale et al., 1997). These observations challenge the hypothesis that the two receptors mobilize different intracellular signaling cascades for acquisition and forgetting.

We have revisited the question of whether the two receptors couple to distinct downstream signaling cascades. We show, using a real-time bioluminescence resonance energy transfer (BRET) assay for G protein activation by G protein coupled receptors (GPCRs) (Masuho et al., 2015b), that dDA1 strongly couples to Gαs and increases cAMP accumulation upon stimulation by DA, whereas the Damb receptor couples preferentially to Gαq over Gαs and induces calcium signaling. Consistent with a Damb/Gαq pathway role in forgetting, RNAi knockdown of Gαq in the MBNs produces a selective deficit in forgetting. These results reconcile the dilemma of how DA stimulates both acquisition and forgetting, with acquisition occurring through a dDA1/Gαs/cAMP pathway and forgetting through Damb/Gαq/Ca<sup>2+</sup>.



(legend on next page)

## RESULTS

### Damb Is a Promiscuous GPCR Preferentially Activating Gq

We first compared the ability of dDA1 and Damb receptors to modulate changes in cAMP and  $\text{Ca}^{2+}$  concentrations in response to DA (Figure 1A). Receptors were reconstituted into HEK293T/17 cells together with firefly luciferase-based GloSensor-22F cAMP sensor (Binkowski et al., 2011) or CalfluxVTN  $\text{Ca}^{2+}$  sensor (Yang et al., 2016), which report real-time fluctuations in second-messenger levels by changes in luminescence and BRET signal, respectively. Consistent with previous reports (Sugamori et al., 1995; Han et al., 1996), we observed that application of DA to cells expressing either dDA1 or Damb stimulated cAMP production (Figure 1B). These responses were driven by the transfected receptors, as no significant signal was observed in control experiments where receptor constructs were omitted. The elevation in cAMP levels was significantly greater in cells transfected with dDA1 compared to those transfected with damb. In contrast, the dDA1 receptor promoted a marginal  $\text{Ca}^{2+}$  response upon DA application, whereas the responses elicited by Damb were robust with fast response kinetics (Figure 1C).

To examine G protein coupling selectivity of the *Drosophila* Damb and dDA1 receptors, we employed a recently developed assay system that directly monitors G protein activation by GPCRs by measuring agonist-induced dissociation of mammalian G protein heterotrimers (Masuho et al., 2015b). In this assay, the release of Venus-tagged  $\text{G}\beta\gamma$  subunits produces BRET responses through interactions with a luciferase-tagged effector mimic, masGRK3ct-Nluc (Figures 1D and 1E). We used the human DA D1 receptor (D1R) as a reference standard for these experiments. Consistent with its well-established mechanism, this receptor elicited responses with large amplitudes via short and long isoforms of  $\text{G}\alpha_s$ , the related  $\text{G}\alpha_{\text{olf}}$ , and the promiscuous G protein  $\text{G}\alpha_{15}$ . Minor coupling was observed to  $\text{G}\alpha_{\text{O}}\text{A}$  and  $\text{G}\alpha_{\text{O}}\text{B}$  (Figure 1F, red wheel diagram). We observed from examining the activation rates, which reflect catalytic efficiency of

GPCRs, that the D1R preferentially activates Gs/Golf over all other G protein substrates (Figure 1F, blue wheel diagram). Our analyses of dDA1 showed similar selectivity to D1R in this assay system employing mammalian  $\text{G}\alpha$  subunits. It activated all Gi/o subunits, G15, and Gs/olf proteins, but the fastest kinetics were found with Gs and Golf. This indicates that the dDA1 receptor behaves in this assay system like a typical mammalian  $\text{G}\alpha$ s-coupled receptor. In contrast, the Damb receptor exhibited a much different coupling profile to human  $\text{G}\alpha$  subunits. It activated Go, Gz, Gq, G11, G14, G15, and Gs/olf proteins to differing extents, but it exhibited the most rapid activation kinetics for Gq and G11.

### Damb and dDA1 Couple Selectively to *Drosophila* $\text{G}\alpha$ Subunits and Differentially Rely on the Chaperone Ric-8 for Function

We next studied the interaction of Damb and dDA1 receptors with native *Drosophila*  $\text{G}\alpha$  subunits using 2  $\text{G}\alpha_{\text{q}}$  proteins,  $\text{G}\alpha_{\text{qD}}$  and  $\text{G}\alpha_{\text{qG}}$ , and 2  $\text{G}\alpha_{\text{s}}$  proteins,  $\text{G}\alpha_{\text{sA}}$  and  $\text{G}\alpha_{\text{sD}}$ . These proteins are isoforms expressed by the two different genes through alternative splicing, and they were identified as being expressed in the brain by cDNA cloning (Table S1). The  $\text{G}\alpha_{\text{sA}}$  isoform was determined to be more abundantly expressed than the  $\text{G}\alpha_{\text{sD}}$  isoform, based on the frequency of clones obtained (Tables S1 and S2). The  $\text{G}\alpha_{\text{qG}}$  isoform was found as more abundantly expressed than the  $\text{G}\alpha_{\text{qD}}$  transcript through qRT-PCR assays (Table S3). First, we examined their expression in HEK293T/17 cells by monitoring their association with mammalian  $\text{G}\beta\gamma$  subunits using a masGRK3ct-Nluc competition assay (Figure 2A). Venus- $\text{G}\beta\gamma$  and masGRK3ct-Nluc form a complex resulting in a large basal BRET signal in the absence of exogenously added  $\text{G}\alpha$  or agonist. Binding of  $\text{G}\alpha$  to  $\text{G}\beta\gamma$  results in a formation of the basal heterotrimeric protein complex, displacing the masGRK3ct-Nluc construct reporter and, thus, reducing the BRET signal. Since the chaperone-like proteins Ric-8A and Ric-8B facilitate the expression of many  $\text{G}\alpha$  subunits (Chan et al., 2013; Gabay et al., 2011; Masuho et al., 2015b), we further studied the effects of their co-expression. We discovered

#### Figure 1. G Protein Selectivity of dDA1 and DAMB

(A) Cartoon of GPCR-mediated second-messenger regulation. Stimulation with agonist leads to charging of the  $\alpha$  subunit with GTP and its dissociation from  $\beta\gamma$  subunits. The  $\text{G}\alpha_{\text{s}}$  subunit stimulates adenylyl cyclase (AC) resulting in cyclic AMP (cAMP) generation, and  $\text{G}\alpha_{\text{q}}$  stimulates phospholipase  $\text{C}\beta$  resulting in calcium release from internal stores.

(B) Cyclic AMP assay to examine Gs coupling of the receptors. HEK293T/17 cells were transfected with GloSensor-22F/cAMP without exogenous GPCR (black) or with dDA1- (cyan) or DAMB- (orange) expressing plasmids. A saturated concentration of DA (100  $\mu\text{M}$ ) was applied at 5 min, and luminescence was monitored for 60 min. Each trace represents the mean of 6 replicates. The bar graph at the right quantitates the relative responses. Statistics: results are expressed as the mean  $\pm$  SEM (ANOVA with Tukey post hoc, \*\*\* $p < 0.001$ ;  $n = 6$  per group).

(C)  $\text{Ca}^{2+}$  assay to examine Gq coupling. HEK293T/17 cells were transfected with CalfluxVTN without exogenous GPCR or with dDA1- or DAMB-expressing cDNAs. 100  $\mu\text{M}$  DA was applied at 5 s and the BRET ratio was monitored for 2 min. Each trace represents the mean of 6 replicates. The bar graph at the right quantitates the relative responses. Statistics: results are expressed as the mean  $\pm$  SEM (ANOVA with Tukey post hoc, \*\*\* $p < 0.001$ ;  $n = 6$  per group).

(D) Schematic representation of the BRET assay for real-time monitoring of G protein activity. Activation of a GPCR by agonist leads to the dissociation of inactive heterotrimeric G proteins into active GTP-bound  $\text{G}\alpha$  and Venus- $\text{G}\beta\gamma$  subunits. The released Venus- $\text{G}\beta\gamma$  can then interact with the  $\text{G}\beta\gamma$  effector mimetic masGRK3ct-Nluc to produce the BRET signal. The masGRK3ct-Nluc reporter protein consists of C-terminal fragment of G protein receptor kinase type 3 (GRK3) fused to a myristic acid attachment peptide (mas) and NanoLuc luciferase (Nluc) attached at the C terminus (ct).

(E) Real-time monitoring of G protein activation by the DAMB receptor. HEK293T/17 cells were transfected with the BRET sensor pair (D) and DAMB together with  $\text{G}\alpha_{\text{O}}\text{A}$  (black),  $\text{G}\alpha_{\text{q}}$  (green), or  $\text{G}\alpha_{\text{sS}}$  (magenta). DA at 100  $\mu\text{M}$  concentration was applied at time zero and the BRET signal was followed across time. This time plot illustrates how the rate and magnitude of G protein coupling were assayed in (F).

(F) G protein selectivity diagrams of the human DA D1 receptor (D1R), dDA1, and DAMB. The maximum amplitudes (red) and activation rate constants (blue) from 14 different G proteins were normalized to the largest value and plotted in the wheel diagrams. Line thickness represents the SEM of six technical replicates performed in parallel. Two biological replicates using independent transfections were performed with similar results. Data are shown from one of the experiments.

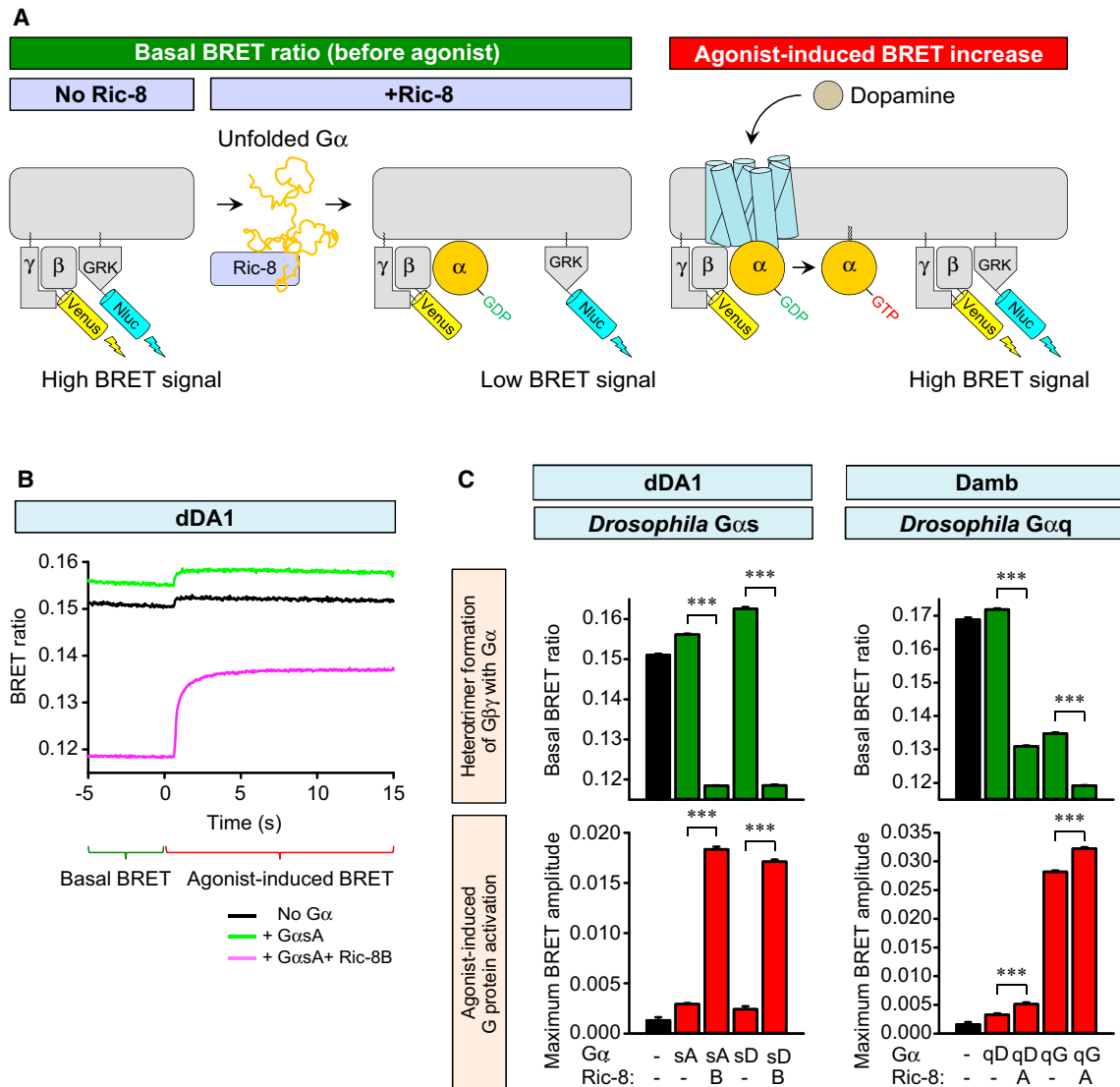


**Figure 2. Effects of Mammalian Ric-8A and Ric-8B on Expression of *Drosophila*  $G\alpha$  Subunits**

(A) Schematic diagram of the Ric-8 effects in BRET assays with and without agonist. Co-transfection of Ric-8 with  $G\alpha$  provided for expression of functional  $G\alpha$  subunits and interaction of  $G\alpha$  with Venus- $G\beta\gamma$ . Functional heterotrimer formation consequently decreased the basal BRET ratio and increased agonist-induced BRET response.

(B) Effect of Ric-8B,  $G\alpha$ sA, and DA on signaling through the dDA1 receptor. HEK293T/17 cells were transfected with the BRET sensor pair and dDA1 without exogenous  $G\alpha$  (black), with  $G\alpha$ sA (green) or  $G\alpha$ sA and Ric-8B (magenta). DA was added at time zero at a concentration of 100  $\mu$ M. Functional  $G\alpha$ sA (with Ric-8A) decreased the basal BRET ratio indicating heterotrimer formation. DA agonist produced a robust and quantifiable response.

(C) Effects of DA, Ric-8A or -8B, and  $G\alpha$ sA,  $G\alpha$ sG,  $G\alpha$ qD, or  $G\alpha$ qG on signaling through the dDA1 and Damb receptors. The cellular BRET assay for the dDA1 receptor was performed with  $G\alpha$ sA and  $G\alpha$ sG (left), with and without Ric-8B, and for the Damb receptor with  $G\alpha$ qD and  $G\alpha$ qG (right), with and without Ric-8A. The basal BRET ratio and agonist-induced maximum response amplitude were plotted as bar graphs. Statistics: results are expressed as the mean  $\pm$  SEM (ANOVA with Tukey post hoc, \*\*\* $p$  < 0.001;  $n$  = 6 per group).

that both  $G\alpha$ sA and  $G\alpha$ sD were able to form complexes with  $G\beta\gamma$  subunits, as indicated by the suppression of the basal BRET signal and that this process strictly required the presence of Ric-8B (Figures 2B and 2C). Similarly, we were able to reconstitute heterotrimeric protein complexes of both  $G\alpha$ qD and  $G\alpha$ qG with  $G\beta\gamma$  subunits. Formation of the heterotrimeric protein complex containing  $G\alpha$ qD required the expression of Ric-8A. Complex formation with  $G\alpha$ qG occurred without the expression of

Ric-8A, but this chaperone further enhanced the formation of the heterotrimer.

When stimulated with DA, the dDA1 receptor supported robust generation of the BRET signal with both  $G\alpha$ sA and  $G\alpha$ sD only in the presence of Ric-8B, indicating the ability of this protein combination to fully support signaling upon activation of the receptor (Figures 2B and 2C). In contrast, only  $G\alpha$ qG supported an increase in BRET signal upon activation of

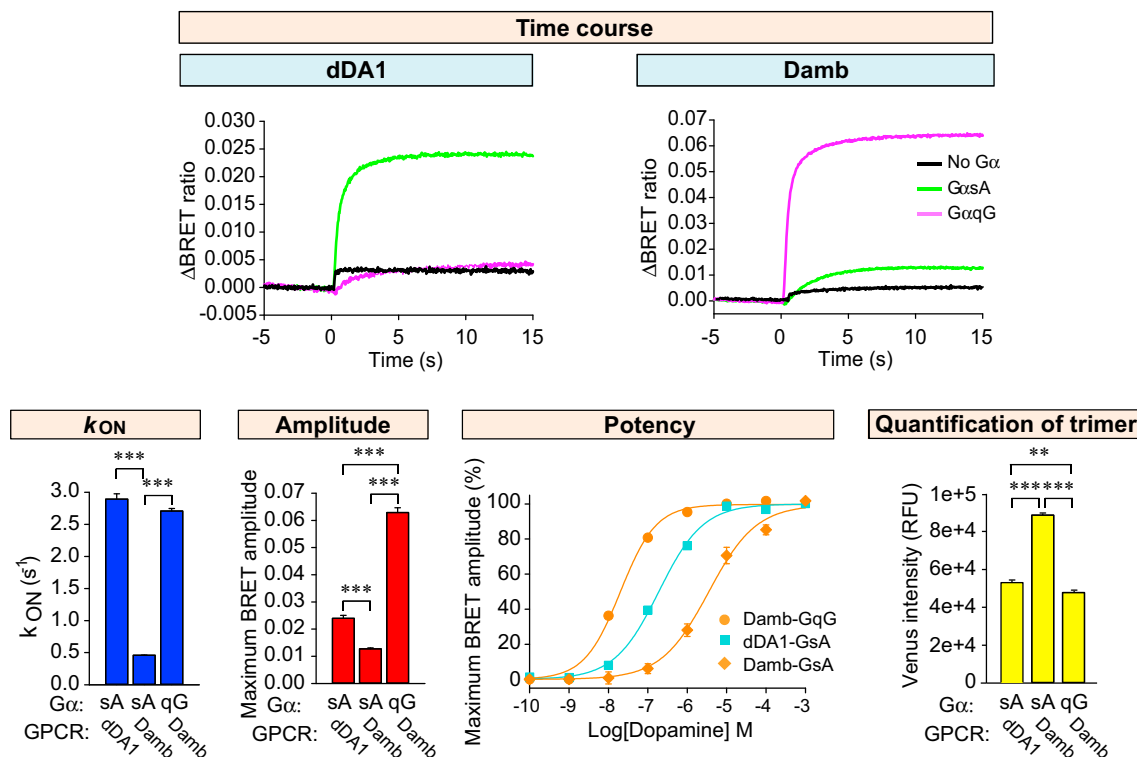


**Figure 3. Biochemical Characterization of dDA1- and DAMB-Mediated Signaling**

Time course of G protein activation mediated by the dDA1 and DAMB receptors shown at the top of the figure. DA at 100  $\mu$ M was applied at time zero. Activation rate constants and agonist-induced maximum BRET amplitudes are plotted as bar graphs. Dose-response analyses were performed for dDA1 with the  $G\alpha SA$  combination and for DAMB with the  $G\alpha SA$  and  $G\alpha qG$  combinations. Statistics: results are expressed as the mean  $\pm$  SEM (ANOVA with Tukey post hoc, \*\*\* $p$  < 0.001;  $n$  = 6 per group). Quantification of trimeric G protein in transfected cells was performed as described in Figure S1C. The intensity of Venus in cells transfected without  $G\alpha$  was subtracted from the intensity in cells transfected with  $G\alpha$ . Statistics: results are expressed as the mean  $\pm$  SEM (ANOVA with Tukey post hoc, \*\* $p$  < 0.01 and \*\*\* $p$  < 0.001;  $n$  = 8 per group).

Damb by DA, and this effect was only slightly potentiated by Ric-8A. Along with results indicating a much higher expression of  $G\alpha qG$  mRNA in the *Drosophila* brain over  $G\alpha qD$ , these results indicate that Damb likely couples primarily to  $G\alpha qG$ .

### Damb- $G\alpha qG$ Is a High-Sensitivity Dopamine Detector

We then compared the responses of Damb and dDA1 to DA with combinations of native *Drosophila*  $G\alpha$  subunits. To enable quantitative comparisons, we first titrated the  $G\alpha$  subunit expression to achieve stoichiometric heterotrimer formation (Figure S1). Under these optimal conditions, the dDA1 receptor supported rapid activation kinetics using  $G\alpha SA$ , but not  $G\alpha qG$  (Figure 3). The Damb receptor supported signaling with both *Drosophila*  $G\alpha qG$  and  $G\alpha SA$ , similar to its signaling with mammalian G proteins (Figure 1), but with very different potencies. The rate of activation was 5-fold faster for  $G\alpha qG$  than for  $G\alpha SA$  ( $2.71 \pm 0.04$  s<sup>-1</sup> and  $0.46 \pm 0.01$  s<sup>-1</sup>, respectively), and the amplitude of the response was 6-fold higher (Figure 3). We further explored the sensitivity of dDA1 and Damb to DA in dose-response experiments. Strikingly, the results revealed that Damb activates  $G\alpha qG$  at a 100-fold lower concentration of DA than  $G\alpha SA$  ( $EC_{50}$  =  $7.37 \pm 0.69$   $\mu$ M for  $G\alpha SA$  and  $56.7 \pm 7.7$  nM for  $G\alpha qG$ ). Furthermore, the potency of Damb- $G\alpha qG$  coupling was an order

of magnitude higher than that of dDA1- $G\alpha SA$  ( $EC_{50}$  =  $0.61 \pm 0.07$   $\mu$ M). Interestingly, at saturating concentrations of DA, Damb and dDA1 elicited responses using  $G\alpha SA$  of similar magnitude, consistent with the substantial cAMP production driven by Damb observed above (Figure 1B). Control experiments measuring the proteolytically stable heterotrimer in transfected cells indicated that differences in expression levels of *Drosophila* receptor/G protein combinations could not account for the differential G protein coupling described above (Figure S1C; Figure 3). Together, these findings establish Damb as a dual-specificity GPCR, signaling primarily through  $GqG$  at low levels of DA and additionally through  $GsA$  at higher levels.

### Knockdown of $G\alpha q$ Leads to Memory Enhancement

We subsequently tested the hypothesis that  $G\alpha q$  mediates the intrinsic forgetting function of the Damb receptor on olfactory memories with Gal4-*uas* RNAi knockdown experiments (Figure 4A). Our initial experiments employed Gal4 lines expressed pan-neuronally or in the MBns, but, using *Nsyb-gal4* (all neurons), *R13-gal4* (MBns), and *c772-gal4* (MBns), we found that adult flies failed to eclose or that they had impaired olfactory learning, consistent with previously reported neurodevelopmental roles for  $G\alpha q$  (Ratnaparkhi et al., 2002). To avoid these



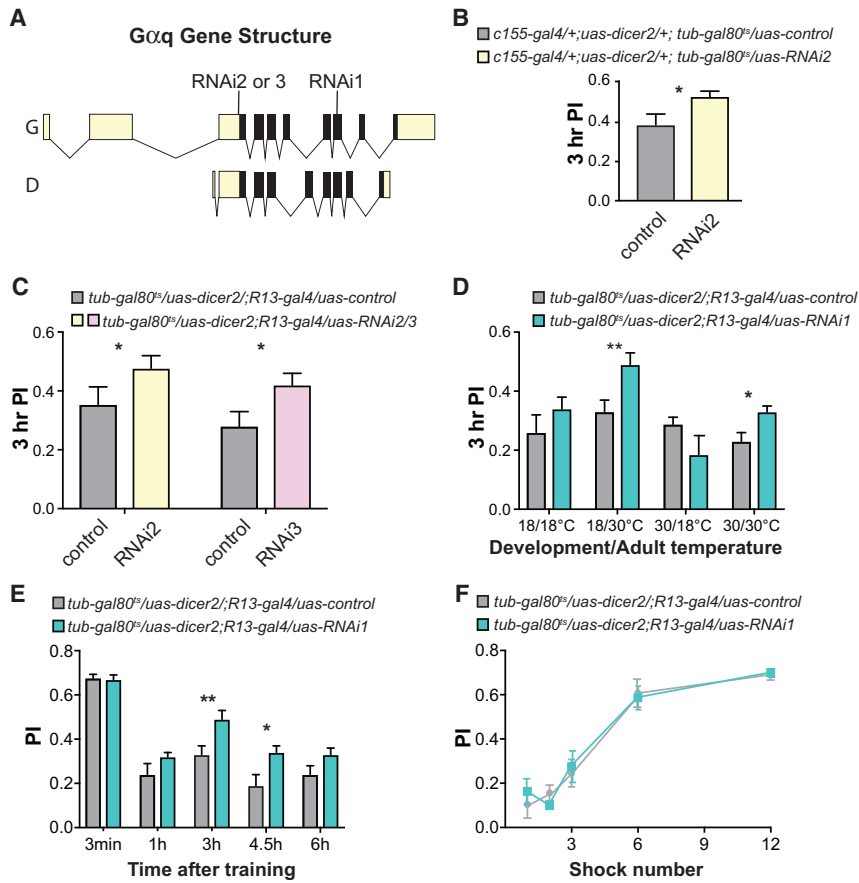


**Figure 4. RNAi Knockdown of  $G_{\alpha q}$  Impairs Forgetting**

(A) The graphic shows the structure of the  $G_{\alpha q}$  gene with two annotated isoforms, G and D. Two different transcriptional units and alternative splicing encode these forms. The open reading frame is illustrated as solid black with 5' and 3' UTRs colored light yellow. Three different RNAi lines were used in this study. All three  $G_{\alpha q}$  RNAi transgenes encode short hairpin RNAi sequences complementary to 24 nt of two annotated isoforms, G and D, with RNAi2 and 3 targeting the 5' UTR in exon 4 and  $G_{\alpha q}$  RNAi1 targeting sequences in exon 10. Figure S3 illustrates an expanded exons 4 and 10 and the specific sequences targeted by the three RNAi lines.

(B) RNAi knockdown of  $G_{\alpha q}$  using the pan-neuronal  $c155\text{-gal4}$  driver and  $tub\text{-gal80<sup>ts</sup>}$  to control expression only during adulthood with a temperature shift from 18°C to 30°C after eclosion. The  $tub\text{-gal80<sup>ts</sup>}$  transgene expresses temperature-sensitive Gal80<sup>ts</sup> protein that inhibits Gal4 activity at 18°C, but not at 30°C. The *tubulin* (*tub*) promoter drives expression of  $gal80<sup>ts</sup>$  in all cells. Knockdown of  $G_{\alpha q}$  with RNAi2 increased memory expression relative to the *uas-control*. The *uas-control* is a chromosome containing the *attP40* docking site used for the insertion of the RNAi constructs. Statistics: results are expressed as the mean  $\pm$  SEM (two-tailed, two-sample Student's *t* test, \**p* < 0.05; *n* = 13 per group). (C) RNAi knockdown of  $G_{\alpha q}$  expression in the MBNs using the *R13-gal4* driver only during adulthood increased memory expression. Statistics: results are expressed as the mean  $\pm$  SEM (two-tailed, two-sample Student's *t* test, \**p* < 0.05 and \*\**p* < 0.001; *n* = 12–16 per group).

(D) RNAi knockdown of  $G_{\alpha q}$  expression only during adulthood with two additional RNAi transgenes increased memory performance. Statistics: results are expressed as the mean  $\pm$  SEM (two-tailed, two-sample Student's *t* test, \**p* < 0.05; *n* = 12 per group).

(E) Memory retention was enhanced with  $G_{\alpha q}$ -RNAi expression in the MBNs only at intermediate time, 3 and 4.5 hr, after conditioning. Statistics: results are expressed as the mean  $\pm$  SEM (two-tailed, two-sample Student's *t* test, \**p* < 0.05 and \*\**p* < 0.01; *n* = 8–12 per group).

(F) RNAi knockdown of  $G_{\alpha q}$  expression in adult MBNs did not alter the memory acquisition curve with flies trained with an increasing number of electric shock pulses. Statistics: results are expressed as the mean  $\pm$  SEM (two-factor ANOVA, not significant [n.s.]; *n* = 6 per group).

developmental complications, we controlled the expression of RNAi transgenes only during adulthood using *tub-gal80<sup>ts</sup>* (Figure 4B; McGuire et al., 2003). Experimental flies expressing  $G_{\alpha q}$  RNAi2 in adult neurons showed an increase in memory of ~30% compared to control flies when tested at 3 hr after conditioning (Figure 4B). We tested two additional  $G_{\alpha q}$  RNAi lines targeting different sequences of  $G_{\alpha q}$  (Figure 4A; Figure S2A) to confirm these behavioral results and to test the role of knockdown in the MBNs. Similar to the results obtained with adult, pan-neuronal expression of RNAi2, knockdown with these RNAis in adult MBNs produced an increase in the performance index, mapping the forgetting deficit to the MBNs and showing that the phenotype observed with RNAi2 was not due to off-target effects (Figure 4C).

We also tested flies expressing the RNAi transgenes in the adult MBNs for possible defects in odor and electric shock avoidance, the two sensory channels for delivering the conditioned stimulus (CS) and US in olfactory classical conditioning. No significant difference was found in avoidance responses between flies expressing the RNAi transgenes in the MBNs compared to

the control genotype relative to either type of stimulus (Figures S2B–S2D), precluding the possibility that the behavioral effects observed were due to altered sensory perception.

Ascribing the forgetting phenotype to insulting  $G_{\alpha q}$  expression in adult MBNs does not eliminate the possibility of an adult behavioral role from developmental expression. We explored this possibility by shifting the incubation temperature of flies to conditionally express  $G_{\alpha q}$  RNAi in MBNs (Figure 4D). While memory was improved with the expression of  $G_{\alpha q}$  RNAi in adult MBNs, expression during development produced a non-significant trend toward impairment (Figure 4D). Thus, the deficit in forgetting ensues from an adult, physiological role for  $G_{\alpha q}$ . We also measured memory expression at multiple times after conditioning to obtain a better understanding of the temporal forms of memory altered by  $G_{\alpha q}$  blockade (Figure 4E). The results indicated that RNAi knockdown had no effect on memory measured immediately or at 1 hr after conditioning. We again observed impaired forgetting at 3 hr after training and at 4.5 hr. These results indicate that forgetting was impaired across a time window typically considered as intermediate-term memory (Davis, 2011).

The magnitude of the observed deficit was more modest than that measured in flies carrying a *damb* mutation (Berry et al., 2012), but this quantitative difference can be accounted for by the greater strength of a genomic null mutation compared to RNAi knockdown.

To test whether the  $G\alpha q$  RNAi knockdown leads to increased acquisition that could produce enhanced memory, we performed acquisition experiments by training flies with an increasing number of shock pulses (Figure 4F). The experimental flies performed equivalently to the controls in this experiment, indicating that acquisition of memory was comparable between the two groups and arguing against increased acquisition as a possible explanation for the enhanced memory observed with  $G\alpha q$  RNAi knockdown.

## DISCUSSION

Here we provide biochemical and behavioral evidence that the *Drosophila* DA receptor Damb couples preferentially to  $G\alpha q$  to mediate signaling by Damb for active forgetting. This conclusion offers an interesting contrast to the role of the dDA1 receptor in MBNs for acquisition, and it resolves the issue of how MBNs distinguish DA-mediated instructions to acquire memory versus those to forget. Prior studies (Sugamori et al., 1995; Han et al., 1996; Reale et al., 1997) had classified both dDA1 and Damb as cAMP-stimulating receptors, similar to mammalian  $D_1/D_5$  DA receptors that work through  $G\alpha s$ /olf. Our results extend prior studies of dDA1 by examining coupling of this receptor with multiple heterotrimeric G proteins to show that the receptor strongly and preferentially couples to Gs proteins. This affirms the receptor's role in the acquisition of memory (Kim et al., 2007), consistent with the tight link between acquisition and cAMP signaling (Davis, 2005; Tomchik and Davis, 2009). We found that the Damb receptor can weakly couple to Gs proteins but preferentially engages Gq to trigger the  $Ca^{2+}$ -signaling pathway, a feature not displayed by dDA1. Comparing the two  $G\alpha q$  paralogs of *Drosophila* (G and D) with a human ortholog shows that *Drosophila*  $G\alpha qG$  and human  $G\alpha q$  share a conserved C terminus, essential for selective coupling to GPCRs, but quite distinct in sequence compared to the  $G\alpha qD$  C terminus (Figure S3). Since  $G\alpha qD$  is a photoreceptor-selective G protein that couples with rhodopsin (Lee et al., 1994), we propose that  $G\alpha qG$  is the isoform that relays Damb's signals to spur forgetting.

We envision that memory acquisition triggered by strong DA release from electric shock pulses used for aversive conditioning drives both cAMP and  $Ca^{2+}$  signaling through dDA1 and Damb receptors in the MBNs (Figure S4). Forgetting occurs from weaker DA release after the acquisition through restricted Damb/ $G\alpha q$ / $Ca^{2+}$  signaling in the MBNs. The coupling of Damb to Gs at high DA concentrations also explains why Damb mutants have a slight acquisition defect after training with a large number of shocks (Berry et al., 2012). Although the model allows the assignment of acquisition and forgetting to two distinct intracellular signaling pathways, it does not preclude the possibility that other differences in signaling distinguish acquisition from forgetting. These include the possible use of different presynaptic signals, such as a co-neurotransmitter released only during acquisition or forgetting.

## EXPERIMENTAL PROCEDURES

### Cell Culture and Transfections

HEK293T/17 cells were seeded and grown for 4 hr prior to transfection with the appropriate constructs. For the cAMP assays, *Drosophila* DA receptor pGloSensor-22F cAMP and PTX-S1 constructs were used. Transfected cells were detached and transferred to microtiter plates containing the GloSensor cAMP Reagent prepared according to the manufacturer's directions. After 2 hr at room temperature, luminescence was monitored continuously with a microplate reader. DA in solvent was then applied to cells. For the  $Ca^{2+}$  assays, *Drosophila* DA receptor CalfluxVTN and PTX-S1 constructs were used. PTX-S1 was co-transfected to inhibit the possible coupling of endogenous Gi/o to DA receptors. This ensures that all signal recorded in these assays is generated exclusively by the activation of Gs or Gq. For the assay, transfected cells were harvested and resuspended in PBS with  $MgCl_2$  and glucose. The cells were distributed in microplates and the Nluc substrate furimazine was added. BRET measurements were made using a microplate reader with the signal calculated by measuring the ratio of the light emitted by the Venus reporter and the Nluc reporter. The average baseline value (basal BRET ratio) recorded prior to agonist stimulation was subtracted from the experimental BRET signal values to obtain the  $\Delta$ BRET ratio. The largest agonist-induced  $\Delta$ BRET ratio was plotted as the maximum BRET amplitude. Cellular measurements of BRET between Venus-G $\beta\gamma$  and masGRK3ct-Nluc were performed (Masuho et al., 2015a, 2015b), with minor modifications to monitor G protein activity in real time with BRET sensors.

### Fly Behavioral Experiments

We used 6-day-old flies for all behavioral experiments. For conditioning, ~60 flies in a conditioning tube received 30 s of fresh air, 1 min of an odor paired with electric shock pulses (CS+), 30 s of air, 1 min of a second odor with no electric shock pulses (CS−), and finally 30 s of air. 3-octanol (OCT) and benzaldehyde (BEN) were used as standard odorants in our experiments. Flies were tested in T-mazes in which they were allowed to choose between the CS+ and CS− presented in two different arms of the maze. Memory was quantified by calculating the performance index (PI) as the (number of flies in the CS− arm) − (number of flies in the CS+ arm)/(number of flies in the CS− arm) + (number of flies in the CS+ arm). Shock and odor avoidance tests were performed on naive flies to control for any possible change in odor/shock perception and avoidance. The TARGET system (McGuire et al., 2003) was used to control *uas-transgene* expression with temperature. This employs constitutive expression of a temperature-sensitive Gal4 inhibitor, Gal80<sup>TS</sup>. The 30°C temperature destabilizes Gal80<sup>TS</sup> and allows Gal4 to drive the expression of the *uas-transgene* present.

### Statistical Analyses

Data were analyzed using Student's t test or ANOVA for multiple group comparisons, as specified in the figure legends.

## SUPPLEMENTAL INFORMATION

Supplemental Information includes Supplemental Experimental Procedures, four figures, and three tables and can be found with this article online at <https://doi.org/10.1016/j.celrep.2017.10.108>.

## AUTHOR CONTRIBUTIONS

Conceptualization, K.A.M. and R.L.D.; Methodology, S.H., I.M., J.A.B., C.M., and N.K.S.; Investigation, S.H., I.M., J.A.B., C.M., and N.K.S.; Supervision, K.A.M. and R.L.D.; Writing – Original Draft, S.H., I.M., K.A.M., and R.L.D.; Writing – Review & Editing, S.H., I.M., J.A.B., C.M., N.K.S., K.A.M., and R.L.D.; Project Administration, K.A.M. and R.L.D.; Funding Acquisition, K.A.M. and R.L.D.

## ACKNOWLEDGMENTS

Research in the Davis laboratory was supported by grants 4R37NS019904, 5R01NS052351, and 1R35NS097224 from NINDS. Research in the



Martemyanov laboratory was supported by grants DA036596 and DA026405 from NIDA, and MH105482 from NIMH. We thank TRiP at Harvard Medical School (NIH/NIGMS R01-GM084947) and Janelia Farms for providing transgenic fly stocks used in this study.

Received: August 17, 2017

Revised: October 4, 2017

Accepted: October 26, 2017

Published: November 21, 2017

## REFERENCES

- Aso, Y., Herb, A., Ogueta, M., Siwanowicz, I., Templier, T., Friedrich, A.B., Ito, K., Scholz, H., and Tanimoto, H. (2012). Three dopamine pathways induce aversive odor memories with different stability. *PLoS Genet.* 8, e1002768.
- Berry, J.A., Cervantes-Sandoval, I., Nicholas, E.P., and Davis, R.L. (2012). Dopamine is required for learning and forgetting in *Drosophila*. *Neuron* 74, 530–542.
- Berry, J.A., Cervantes-Sandoval, I., Chakraborty, M., and Davis, R.L. (2015). Sleep facilitates memory by blocking dopamine neuron-mediated forgetting. *Cell* 161, 1656–1667.
- Binkowski, B.F., Butler, B.L., Stecha, P.F., Eggers, C.T., Otto, P., Zimmerman, K., Vidugiris, G., Wood, M.G., Encell, L.P., Fan, F., and Wood, K.V. (2011). A luminescent biosensor with increased dynamic range for intracellular cAMP. *ACS Chem. Biol.* 6, 1193–1197.
- Chan, P., Thomas, C.J., Sprang, S.R., and Tall, G.G. (2013). Molecular chaperoning function of Ric-8 is to fold nascent heterotrimeric G protein  $\alpha$  subunits. *Proc. Natl. Acad. Sci. USA* 110, 3794–3799.
- Claridge-Chang, A., Roorda, R.D., Vrontou, E., Sjulson, L., Li, H., Hirsh, J., and Miesenböck, G. (2009). Writing memories with light-addressable reinforcement circuitry. *Cell* 139, 405–415.
- Davis, R.L. (2005). Olfactory memory formation in *Drosophila*: from molecular to systems neuroscience. *Annu. Rev. Neurosci.* 28, 275–302.
- Davis, R.L. (2011). Traces of *Drosophila* memory. *Neuron* 70, 8–19.
- Davis, R.L., and Zhong, Y. (2017). The Biology of Forgetting—A Perspective. *Neuron* 95, 490–503.
- Gabay, M., Pinter, M.E., Wright, F.A., Chan, P., Murphy, A.J., Valenzuela, D.M., Yancopoulos, G.D., and Tall, G.G. (2011). Ric-8 proteins are molecular chaperones that direct nascent G protein  $\alpha$  subunit membrane association. *Sci. Signal.* 4, ra79.
- Han, K.A., Millar, N.S., Grotewiel, M.S., and Davis, R.L. (1996). DAMB, a novel dopamine receptor expressed specifically in *Drosophila* mushroom bodies. *Neuron* 16, 1127–1135.
- Kim, Y.C., Lee, H.-G., Seong, C.-S., and Han, K.-A. (2003). Expression of a D1 dopamine receptor dDA1/DmDOP1 in the central nervous system of *Drosophila melanogaster*. *Gene Expr. Patterns* 3, 237–245.
- Kim, Y.C., Lee, H.G., and Han, K.A. (2007). D1 dopamine receptor dDA1 is required in the mushroom body neurons for aversive and appetitive learning in *Drosophila*. *J. Neurosci.* 27, 7640–7647.
- Lee, Y.J., Shah, S., Suzuki, E., Zars, T., O'Day, P.M., and Hyde, D.R. (1994). The *Drosophila* dgq gene encodes a G alpha protein that mediates phototransduction. *Neuron* 13, 1143–1157.
- Masuh, I., Martemyanov, K.A., and Lambert, N.A. (2015a). Monitoring G Protein Activation in Cells with BRET. *Methods Mol. Biol.* 1335, 107–113.
- Masuh, I., Ostrovskaya, O., Kramer, G.M., Jones, C.D., Xie, K., and Martemyanov, K.A. (2015b). Distinct profiles of functional discrimination among G proteins determine the actions of G protein-coupled receptors. *Sci. Signal.* 8, ra123.
- McGuire, S.E., Le, P.T., Osborn, A.J., Matsumoto, K., and Davis, R.L. (2003). Spatiotemporal rescue of memory dysfunction in *Drosophila*. *Science* 302, 1765–1768.
- Ratnaparkhi, A., Banerjee, S., and Hasan, G. (2002). Altered levels of Gq activity modulate axonal pathfinding in *Drosophila*. *J. Neurosci.* 22, 4499–4508.
- Reale, V., Hannan, F., Hall, L.M., and Evans, P.D. (1997). Agonist-specific coupling of a cloned *Drosophila melanogaster* D1-like dopamine receptor to multiple second messenger pathways by synthetic agonists. *J. Neurosci.* 17, 6545–6553.
- Schroll, C., Riemensperger, T., Bucher, D., Ehmer, J., Völler, T., Erbguth, K., Gerber, B., Hendel, T., Nagel, G., Buchner, E., and Fiala, A. (2006). Light-induced activation of distinct modulatory neurons triggers appetitive or aversive learning in *Drosophila* larvae. *Curr. Biol.* 16, 1741–1747.
- Schwaerzel, M., Monastirioti, M., Scholz, H., Friggi-Grelin, F., Birman, S., and Heisenberg, M. (2003). Dopamine and octopamine differentiate between aversive and appetitive olfactory memories in *Drosophila*. *J. Neurosci.* 23, 10495–10502.
- Sugamori, K.S., Demchishyn, L.L., McConkey, F., Forte, M.A., and Niznik, H.B. (1995). A primordial dopamine D1-like adenylyl cyclase-linked receptor from *Drosophila melanogaster* displaying poor affinity for benzazepines. *FEBS Lett.* 362, 131–138.
- Tomchik, S.M., and Davis, R.L. (2009). Dynamics of learning-related cAMP signaling and stimulus integration in the *Drosophila* olfactory pathway. *Neuron* 64, 510–521.
- Yang, J., Cumberbatch, D., Centanni, S., Shi, S.Q., Winder, D., Webb, D., and Johnson, C.H. (2016). Coupling optogenetic stimulation with NanoLuc-based luminescence (BRET) Ca(++) sensing. *Nat. Commun.* 7, 13268.